Global J. Environ. Sci. Manage. 13(1): 189-212, Winter 2027, Serial #49

Global Journal of Environmental Science and Management
(GJESM)

Homepage: https://www.gjesm.net/

Podcasts

CASE STUDY

Inflow modeling strategies designed to enhance the ecological sustainability of hydroelectric reservoir operation planning

I. Mulyawati[1], I.R.S. Salami[2,*], M. Marselina[2], A. Sabar[2,3]

[1]Environmental Engineering Graduate Program, Faculty of Civil and Environmental Engineering, Institut Teknologi Bandung, Bandung 40132 Indonesia

[2]Department of Environmental Engineering, Faculty of Civil and Environmental Engineering, Institut Teknologi Bandung, Bandung 40132 Indonesia

[3]Department of Environmental Engineering, Faculty of Infrastructure and Regional Technology, Institut Teknologi Sumatera, South Lampung 35365 Indonesia

ARTICLE INFO

Article History:
Received 03 May 2026
Revised 17 July 2026
Accepted 18 August 2026

Keywords:
Environmental flows
Inflow forecasting
Karian Reservoir
Markov Chain
Monsoonal tropics
Multiple linear regression

ABSTRACT

BACKGROUND AND OBJECTIVES: The rapid global expansion of water infrastructure alters major rivers, causes severe biodiversity declines, and destabilizes aquatic ecosystems. Amid intensifying eco-hydrological pressures, accurate prediction of reservoir inflow remains imperative to safeguard downstream aquatic ecosystems, yet data-sparse tropical environments chronically impair the generalizability of deep learning architectures due to pronounced overfitting. The study objectives were to evaluate three statistical inflow modeling frameworks, representative of design-era hydrological understanding, against the observed 1998–2023 flow regime to identify the most reliable forecasting approach for supporting environmental-flow-informed reservoir operation planning under monsoonal variability.

METHODS: Using a multi-decadal hydro-meteorological dataset from 1998 to 2023 (n = 312 monthly time steps) at Karian Reservoir in Banten Province, Indonesia, three primary modeling approaches were tested: Autoregressive Integrated Moving Average, Markov Chain, and Multiple Linear Regression. To rigorously assess model diagnostics and predictive performance across historical drought and wet regimes, the Pearson correlation coefficient, Kling-Gupta efficiency, and operational trajectory metrics were integrated.

FINDINGS: Deterministic multiple linear regression achieved the highest overall predictive accuracy with a Pearson correlation coefficient of 0.74, a Kling-Gupta efficiency of 0.64, and a superior operational trajectory guideline correlation of 0.85. The observed enhancement in model efficacy stems from the methodical integration of lagged streamflow predictors that effectively characterize catchment-scale moisture persistence. Conversely, the Autoregressive Integrated Moving Average model exhibited the weakest diagnostic capability (Pearson correlation coefficient = 0.62; Kling-Gupta efficiency = 0.60) due to systematic overestimation of dry-season baseflows, risking artificial inflation of safe water availability. Meanwhile, the stochastic Markov yielded a commensurate aggregate Kling-Gupta efficiency score of 0.66 and exhibited a superior proficiency in replicating long-term probability distributions.

CONCLUSION: While Multiple Linear Regression shows the strongest performance for monthly operational scheduling, the Markov Chain model offers a complementary probabilistic framework for screening extended seasonal drought risk. Independent out-of-sample validation against a held-out 2019–2023 period revealed substantial performance degradation for both models (Multiple Linear Regression Nash-Sutcliffe efficiency declining from 0.61 to 0.02; Markov Chain Nash-sutcliffe efficiency declining from 0.28 to -1.01), directly evidencing non-stationary rainfall-inflow relationships. Ultimately, these results establish that the evaluated models serve as an initial decision-support tool for raw water allocation planning, though their sustained operational reliability necessitates systematic recalibration.

DOI:10. 22034.gjesm.2027.01.09

This is an open access article under the CC BY license (http://creativecommons.org/licenses/by/4.0/)

NUMBER OF REFERENCES	NUMBER OF FIGURES	NUMBER OF TABLES
63	9	3

*Corresponding Author:
Email: indahrss@itb.ac.id
Phone: +628170292093
ORCID: 0000-0003-4108-1110

Note: Discussion period for this manuscript open until March 01, 2027 on GJESM website at the “Show Article”.

INTRODUCTION

A reservoir is an engineered ecological system whose operation governs downstream hydrological regimes, aquatic habitat continuity, and riparian ecosystem health (Chan *et al*., 2025). Global water-infrastructure expansion has altered more than two-thirds of the world's large rivers, precipitating biodiversity declines and destabilizing deltaic environments (Grill *et al*., 2019). Integrating hydrological forecasting with reservoir operation reinforces overall system performance and protects downstream aquatic ecosystems by substituting inflexible release rules with dynamic, environmentally responsive strategies (Zarei *et al*., 2021). Accurate inflow forecasting directly underpins outflow discharge calculations, storage stability, and environmental flow delivery, especially as anthropogenic climate change alters basin-scale hydrological regimes (Jayanti *et al*., 2025; Null *et al*., 2024; Anand and Oinam, 2019). Despite advances in deep learning for streamflow prediction, robust statistical models—namely multiple linear regression (MLR), Markov chain, and autoregressive integrated moving average (ARIMA)—remain widely preferred in data-scarce tropical regions where complex black-box models often overfit limited records and lack physical interpretability (Hasan *et al*., 2025; Dimitriadou and Nikolakopoulos, 2022; Gupta and Kumar, 2022). A salient manifestation of this challenge is observed in the Karian Reservoir—a multipurpose engineering project in Banten Province, Indonesia—that mirrors the intricate eco-hydrological trade-offs inherent to large-scale tropical reservoirs (Wahyono *et al*., 2026). Karian must simultaneously fulfill five Phase 1 operational objectives: urban raw water supply, Ciujung River irrigation, municipal releases, run-of-river hydropower, flood control, and a minimum environmental flow of 3.06 m^3/s (Mulyawati *et al*., 2024; BBWS C3, 2025). At 24% of mean annual flow, this environmental release meets the Tennant (1976) "satisfactory" threshold during the wet season but falls below "fair" in the dry season. Legally, Indonesian regulations mandate incorporating river-maintenance flow into every dam's operating pattern, tied to the Q95% dependable discharge (Government of Indonesia, 2011; Ilmi, 2022). Critically, Karian's target releases were derived from a Q355 low-flow index computed from 1970–2004 hydrological records (KOICA, 2006). This epoch precedes both significant upstream land-use transformations (18.3% since 2000) (Arianti *et al*., 2015) and documented ENSO-driven rainfall shifts (Aldrian and Dwi Susanto, 2003). The obsolescence of traditional design-era assumptions under evolving hydrological regimes has received global attention via climate modeling; nonetheless, empirical testing against multi-decadal observational records is notably deficient (Yang *et al*., 2017; Yang *et al*., 2021; Mazvimavi *et al*., 2024). Furthermore, prior evaluations of Indonesian multipurpose reservoirs like Citarum (Arwin and Bourqueil, 1992) and Saguling (Marselina *et al*., 2017) evaluated operating policies under baseline hydrology without testing whether historical forecasting models remain valid decades later. A unique circumstance at Karian is that while inaugurated in 2024 for flood control and irrigation, its full raw water supply function targeting Jabodetabek will only be complete by 2027. Thus, no direct operational record exists. To address this, the 1998–2023 inflow series in this study was retrospectively reconstructed via hydraulic routing from continuous long-term gauging stations. Additionally, unlike existing literature emphasizing economic priorities, the present investigation examines the four primary competing demands—hydropower, raw water supply, irrigation, and environmental flow—with equal weighting. Existing literature comparing ARIMA, Markov Chain, and MLR typically evaluates forecast accuracy alone (Mulyawati *et al*., 2025; Magar and Jothiprakash, 2011; Margini *et al*., 2022) or omits explicit environmental-flow thresholds in multi-objective operational

simulations (Jayanti *et al*., 2025). This study bridges the identified knowledge gap by undertaking a systematic benchmark evaluation of the three data-sparse statistical models using the multi-decadal (1998–2023) reconstructed hydrological sequence of the Karian Reservoir. Model performance was evaluated using the Pearson correlation coefficient (r), Nash-sutcliffe efficiency (NSE), and Kling-Gupta Efficiency (KGE). Propagating these predictive outputs through a reservoir operational model allows for an assessment of whether design-era environmental thresholds remain hydrologically defensible amid current monsoonal regimes, cross-validated using Tennant's (1976) methodology. This study aims to identify the most reliable inflow forecasting method for supporting environmental-flow-informed, multi-sectoral reservoir operation planning under a shifted monsoonal hydrological regime. This study has been conducted in the Karian Reservoir watershed in Banten Province, Indonesia, in 2023.

MATERIALS AND METHODS

Study area

This study was conducted at the Karian Reservoir, located in Sajira District, Lebak Regency, Banten Province, Indonesia (Fig. 1). The reservoir has an effective storage capacity of 207 million cubic meter (Mm^3) and drains water from a watershed area of approximately 288 square kilometers (km^2), most of which is fed by the Ciberang River. Based on continuous monthly hydrological records from 1998 to 2023 (n = 312 monthly time steps), the mean annual flow (MAF) was determined to be 12.81 m^3/s (Table 1) (Atieh *et al*., 2017). Key temporal hydrological metrics, such as flow duration curve (FDC) quantiles, extreme discharge months, and inter-annual variability observed in January, are consolidated in Table 1 to maintain narrative conciseness. This pattern of strong monsoonal seasonality and inter-annual variability is consistent with the influence of climate variability driven by the ENSO (Aldrian and Dwi Susanto, 2003). The reliable water discharge of 9.51 m^3/s is fully allocated to various downstream sectors, leaving no operational margin. Consequently, the design water discharge for drought conditions of 4.0 m^3/s obtained from historical feasibility studies (KOICA, 2006; BBWS C3, 2025) sets the benchmark for ecological planning. This threshold assumes heightened significance during arid periods, when discrepancies between managed discharge volumes and required environmental flows yield the most pronounced ecological impairment (Sedghi-Asl and Poursalehan, 2025).

Data collection and preprocessing

Secondary multi-decadal hydrological records (1997–2023) were retrieved from the Korea International Cooperation Agency (KOICA) and Balai Besar Wilayah Sungai Cidanau-Ciujung-Cidurian (BBWS C3). The compiled dataset encompasses daily and monthly reservoir surface elevations, inflow discharges, and spatial rainfall from six monitoring stations: P1 (Banjar Irigasi), P2 (Ciminyak Cilaki), P3 (Sampang Peundeuy), P4 (Sajira), P5 (Cimarga), and P6 (Pasir Ona). Gaps in precipitation records were reconstructed via the continuous imputation technique formulated by Arwin and Bourqueil (1992). Candidate donor stations were identified via Thiessen polygon proximity, and multi-variable regression combinations (2 to 4 variables) yielding the highest coefficient of determination (R^2) were selected to construct a gap-free time series (Qiu *et al*., 2024). Although raw records span 1997–2023 (n = 324 monthly steps), the year 1997 was used exclusively to calculate lag-1 predictors (P1 at t-1, P4 at t-1, and Qin at t-1), required for MLR, ARIMA, and Markov Chain models. This yielded a robust, highly effective calibration and continuous long-term forecasting period of 1998–2023 (n = 312). To verify the long-term data consistency and homogeneity of the datasets, the double mass curve approach (Sriwongsitanon *et al*., 2023) was implemented, and spatial mean areal rainfall was determined through Thiessen polygon interpolation.

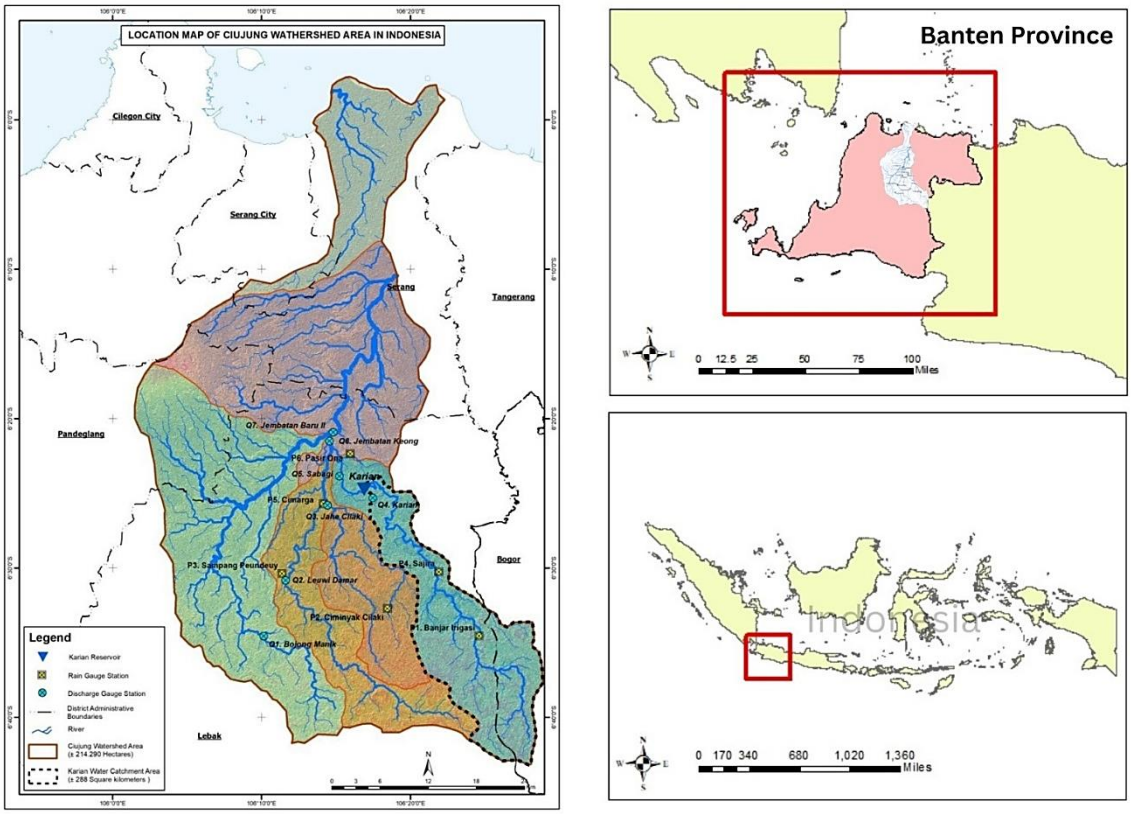

Fig. 1: Geographical location of the study area in the Karian Reservoir watershed in Banten Province, Indonesia, showing the downstream Ciujung River system and the spatial distribution of the hydro-meteorological monitoring network (six rainfall stations, P1-P6) across the 288 km2 Ciberang sub-watershed draining into the 207 million m³ Karian Reservoir

Table 1: Summary of monthly and inter-annual hydrological statistics for Karian Reservoir (1998-2023, n=312)

Statistic	Value
Mean annual flow	12.81 m^3/s
Q80 (flow duration curve quantile)	9.51 m^3/s
Q90 (flow duration curve quantile)	7.67 m^3/s
Highest monthly mean discharge	February: 23.04 m^3/s
Lowest monthly mean discharge	September: 7.53 m^3/s
Most extreme inter-annual range (single month)	January: 1.18-45.61 m^3/s

Due to the absence of a direct gauging station at the reservoir inlet and the ongoing operational ramp-up (with raw water completion targeted for 2027), a synthetic inflow baseline (Q_{in}) was reconstructed from downstream reference stations Q_5 (Sabagi) and Q_7 (Jembatan Baru II) via contemporaneous MLR (Mulyawati *et al.*, 2024). Unlike the lag-1 predictive models, this baseline reconstruction is executed without any underlying lag architecture. For the 1997–2004 period, this reconstructed series showed strong agreement with KOICA's original area-ratio-scaled estimates (Pearson r = 0.916, R^2 = 0.840; Evans, 1996), confirming methodological consistency with design-era baselines. Building upon prior investigations within the catchment (Mulyawati *et al.*, 2025), this comprehensive study directly extends previous work through three key methodological advancements:

1. Standardizing rainfall imputation across all six stations via multiple linear regression.

2. Expanding model performance evaluation to include RMSE, MAE, NSE, MAPE, moving-block bootstrap confidence intervals, and paired-sample significance tests.
3. Propagating forecasts into a full reservoir operation simulation to evaluate environmental-flow target adequacy.

To preserve the integrity of the observational record, extreme hydrological anomalies (such as January inflow rates varying between 1.18 to 45.61 m^3/s) were retained unconditionally, omitting any data capping or exclusion. Preserving this full inter-annual variability was essential to reliably parameterize Weibull-based hydrologic year—categorized as dry, normal, and wet, thereby enabling a realistic representation of operational drought and flood risks in the monsoonal modeling framework simulation.

Flow estimation models

Three robust statistical inflow modeling approaches were evaluated within a unified comparative framework using the quality-controlled dataset (1998–2023, n = 312).

MLR

The MLR model established an explicit linear relationship between contemporary reservoir inflow and antecedent hydro-meteorological predictors (Bargam *et al*., 2024). To accommodate seasonal non-stationarity in the rainfall-inflow relationship, and consistent with the month-specific structure adopted for the Markov Chain transition probabilities and inherent to the seasonal ARIMA specifications the MLR model was parameterized monthly. This generated twelve coefficient sets with uniform predictor architectures but varying numerical values. A pooled-coefficient benchmark demonstrated markedly inferior efficacy (r = 0.40, NSE = 0.16, compared to r = 0.74, NSE = 0.54 in Table 2), validating the month-stratified strategy. Implications regarding the reduced per-month sample size (n = 26-27 years per month) are evaluated in the Discussion. The predictor selection itself was based on upstream spatial positioning and physical hydrological connectivity. These formulations retained three lagged predictors—$P1_{t-1}$ (Banjar Irigasi rainfall), $P4_{t-1}$ (Sajira rainfall), and Qin_{t-1} (lagged inflow), using Eq. 1 (Bargam *et al*., 2024):

$$Q_{in,t} = \beta_0 + \beta_1 P1_{t-1} + \beta_2 P4_{t-1} + \beta_3 Q_{in,t-1} + \epsilon_t \quad (1)$$

Where: β_0 is the intercept, β_1 to β_3 are the partial regression coefficients, and ϵ_t represents the residual error term at time step t.

Markov chain model

Framed as a discrete, stochastic lag-1 process, the Markov chain model parameterized monthly inflows into three discrete states of dry, normal, and wet, using historical monthly distribution quantiles. Following the methodology of Aksoy (2003) as extended in contemporary infrastructure management, month-specific transition probabilities were computed to capture seasonal shifts in transition behavior (Rezaeianzadeh *et al*., 2016; Jayanti *et al*., 2025). The transition probability P_{ij} from state i to state j was mathematically derived using Eq. 2 (Aksoy, 2003):

$$P_{ij} = \frac{n_{ij}}{\sum_{j=1}^{m} n_{ij}} \quad (2)$$

Where: n_{ij} represents the observed historical transitions from state i to state j, and m denotes the total number of defined states (m = 3).

ARIMA model

The ARIMA model exploited the internal autocorrelation structure of the time series. The general model is formulated as $\phi(B)(1-B)^d Q_{in,t} = \Theta(B)\epsilon_t$, where $\phi(B)$ is the autoregressive operator of order p, Θ(B) is the moving average operator of order q, B is the backshift operator ($BX_t = X_{t-1}$), and d is the order of non-seasonal differencing required to achieve stationarity. The optimal

seasonal ARIMA $(p,d,q)(P,D,Q)_s$ structure was rigorously identified via autocorrelation function (ACF) and partial autocorrelation function (PACF) evaluation, minimizing the Akaike information criterion (AIC) (Box *et al*., 2015).

Weibull classification, operation trajectories, and reservoir simulation

The classification of annual inflow volumes into dry, normal, and wet hydrological years was performed using the Weibull plotting position method, thereby facilitating the derivation of return periods and dependability thresholds. Operation guideline trajectories were subsequently derived from a deterministic Rippl Method mass-balance reservoir simulation, using Eq. 3 (Rippl, 1883; Alrayess *et al*., 2017):

$$S_{t-1} = S_t + Q_{in,t} - Q_{out,t} - E_t \quad (3)$$

Where: S_t is the active reservoir storage at month t, constrained strictly between the dead storage level and the 207 million m^3 maximum capacity; $Q_{in,t}$ is the modeled or observed monthly inflow; $Q_{out,t}$ is the total managed outflow release; and E_t represents net evaporative and seepage losses, with long-term active capacity also contingent on catchment sediment yield into the impoundment (Aness *et al*., 2026).

The upper storage boundary (Q_{max} stock) used in the simulation was conservatively set at 200 million m^3, marginally below the reservoir's nominal effective capacity of 207 million m^3, as a simplifying assumption for the statistical simulation exercise. The allocation scheme designated the Tangerang raw water supply as an inflexible, high-priority diversion (6.45 m^3/s) for the duration of every computational time step. Environmental flow performance within $Q_{out,t}$ was dynamically evaluated against the seasonal eco-hydrological thresholds established by the Tennant (1976) method to quantify the ecological reliability of each modeling approach (McMahon and Adeloye, 2005; Shekohideh *et al*., 2026). In fulfillment of the required operational-algorithm specifications for the reservoir simulation, the conversion of operational guidelines into actual implementation followed a two-stage recursive monthly mass-balance procedure. In the first stage, the target (guideline) release T(t) required to keep the reservoir exactly on its Weibull-derived guideline storage trajectory was back-calculated for each month using Eq. 4 (Arwin and Bourqueil, 1992; Loucks and van Beek, 2017; Marselina *et al*., 2016):

$$T(t) = S(t) - Sguideline(t+1) + Qanticipated(t) - E(t) \quad (4)$$

Where: S(t) is the storage carried over from the previous month, Sguideline(t+1) is the target storage prescribed by the applicable reliability-class guideline trajectory for month t+1, Qanticipated(t) is the inflow anticipated for month t from the model under evaluation (ARIMA, Markov Chain, or MLR), and E(t) is net evaporative and seepage loss.

During the second stage, the release T(t) derived from Eq. 4 was held constant while the anticipated inflow was replaced by the actual historical or synthetic inflow Qactual(t), was substituted for the expected inflow to compute the corresponding actual storage through Eq. 5 (Arwin and Bourqueil, 1992; Loucks and van Beek, 2017; Marselina *et al*., 2016):

$$Sactual(t+1) = S(t) + Qactual(t) - T(t) - E(t) \quad (5)$$

The resulting Sactual(t+1) then replaces S(t) as the initial condition for the following month's calculation (Eq. 5 recomputed for month t+1), and the two-stage procedure (Eqs. 4 and 5) is applied recursively across the full 1998-2023 simulation horizon, separately for each of the three inflow models. The proposed recursive coupling serves as the propagation of forecast errors within the reservoir system. Specifically, the release policy is dictated by the guideline trajectory coupled with

the projected inflow, whereas the physical storage dynamics are governed by the realized inflow. Thus, trajectory discrepancies observed in Figs. 7 to 9 serve as a direct measure of the monthly forecast error inherent in the inflow-prediction model. Instead of utilizing a formal multi-objective optimization algorithm (such as dynamic or linear programming), the reservoir simulation framework presented in the Results and Discussion relies on this procedure to define operational constraints and decision rules. This approach was deliberately chosen to evaluate the performance of legacy operating assumptions under historical inflow regimes rather than to derive an optimized release policy—an objective reserved for subsequent research.

Model performance evaluation

Model diagnostic accuracy was systematically validated utilizing r and the modified KGE framework (Gupta *et al*., 2009; Mitze *et al*., 2025). The KGE metric decomposes model performance across three mathematical dimensions: linear correlation (r), bias ratio (β), and variability ratio (γ). A KGE = 1 indicates a perfect match between simulated (s) and observed (o) values, while KGE ≥ 0.75 signifies a highly satisfactory predictive capability, using Eq. 6 (Gupta *et al*., 2009; Mitze *et al*., 2025):

$$r = \frac{[n \cdot \Sigma QoQs - \Sigma Qo \cdot \Sigma Qs]}{\sqrt{[n \cdot \Sigma Qo^2 - (\Sigma Qo)^2][n \cdot \Sigma Qs^2 - (\Sigma Qs)^2]}}$$

$$KGE = 1 - \sqrt{[(r-1)^2 + (\beta-1)^2 + (\gamma-1)^2]} \quad (6)$$

Where: $\beta = \mu_s/\mu_0$ (the ratio of simulated and observed means) and $\gamma = CV_s/CV_o = (\sigma_s/\mu_s)/(\sigma_o/\mu_o)$ (the ratio of simulated and observed coefficients of variation).

The bias ratio (β) component of KGE has direct practical significance for environmental-flow reliability independent of the aggregate KGE score: a model with β > 1 systematically overestimates available discharge, creating the false operational safety margin discussed for ARIMA below, whereas β < 1 would systemacally understate available water and could trigger unnecessarily conservative curtailment; either bias directly affects whether the mandated 3.06 m^3/s environmental release is reliably met, regardless of the model's overall KGE value. In order to enhance the r and KGE metrics and to respond to the reviewers' concerns about the thoroughness of the statistical analysis, four supplementary error metrics were calculated for each model: the root mean square error (RMSE), the mean absolute error (MAE), the NSE, and the mean absolute percentage error (MAPE), in accordance with the methodologies outlined by Moriasi *et al*. (2007) and Lewis (1982). RMSE and MAE quantify the average magnitude of prediction error in the original discharge units (m^3/s), NSE expresses model skill relative to the observed mean as a naive predictor (NSE > 0.5 considered satisfactory), and MAPE expresses the average relative error as a percentage. The RMSE-observations standard deviation ratio (RSR = RMSE/SD of observed values) was additionally computed to classify overall model performance (RSR <= 0.7 considered satisfactory; Moriasi *et al.,* (2007). In addition to point-accuracy metrics, the statistical significance of deviations between the simulated inflow series and the historical (Q_4synthetic) inflow series was rigorously evaluated for each model. Because a Shapiro-Wilk normality test rejected the assumption of normally distributed residuals for all three models ($p < 0.001$), both a parametric paired t-test and a non-parametric Wilcoxon signed-rank test were applied, testing the null hypothesis that no systematic difference exists between simulated and historical inflow values at alpha = 0.05, with the non-parametric result treated as the primary evidence given the non-normal residual distribution. Uncertainty in the reported performance metrics was further quantified using a moving block bootstrap procedure (Künsch, 1989), rather than conventional independent-and-identically-distributed (IID) resampling, because

monthly inflow records exhibit pronounced seasonal autocorrelation that i.i.d. resampling would disrupt, artificially narrowing the estimated uncertainty. For each model, 2,000 bootstrap replicates of the 312-month record were generated by resampling contiguous 12-month blocks with replacement (preserving the annual wet-dry seasonal cycle within each block), and r, KGE, RMSE, MAE, NSE, and MAPE were recalculated for every replicate. The 2.5th and 97.5th percentiles of each resulting bootstrap distribution were taken as the 95% confidence interval (CI) for that metric. Statistical robustness for pairwise model comparisons was established solely in the absence of 95% Cis. Conversely, overlapping intervals suggest that apparent variations in point estimates cannot be separated from sampling uncertainty across the 26-year monthly time series.

RESULTS AND DISCUSSION

This study regularly evaluates the predictive performance of the three dynamic inflow modeling approaches and dissects their operational implications for the Karian reservoir system. The empirical findings are structured to present a comparative statistical validation of the ARIMA, Markov chain, and MLR models, followed by a non-parametric analysis of reliable discharges and reservoir storage trajectories. Finally, this chapter examines the downstream propagation of forecasting variances within long-term multi-objective optimization frameworks, culminating in strategic perspectives for environmentally sustainable water resource governance amidst monsoonal climate shifts.

ARIMA model performance

Performance evaluation of the ARIMA model demonstrated intrinsic structural deficiencies in representing highly dynamic tropical streamflow regimes. The predictive capability of the ARIMA model, alongside the comparative statistical performance metrics of all evaluated frameworks, is summarized in Table 2. As indicated by the statistical criteria, the ARIMA model achieved a correlation coefficient (r) of 0.62 and a KGE of 0.60, exhibiting the weakest overall predictive performance among the three paradigms. To assess the temporal fidelity of the model across sequential time steps, Fig. 2 illustrates a multi-decadal comparison between the reconstructed historical streamflow and the corresponding ARIMA forecasts. As visible in Fig. 2, the ARIMA model systematically compresses predicted peak discharges during the November-March wet season and persistently overestimates baseflows during the June-October dry season. This behavior arises from ARIMA's reliance on stationary linear combinations of past errors and lagged observations, a mechanism that attenuates the non-linear hydrologic extremes induced by monsoonal shifts. In tropical catchments like the Ciberang basin, dry-season baseflows are sustained predominantly by groundwater recession rather than immediate atmospheric forcing, a physical process whose dynamics cannot be effectively decoupled by the stationary stochastic framework of the ARIMA model from rapid monsoonal transitions occurring in April and October. This systematic dry-season overestimation creates a false sense of water availability: when integrated into the Rippl mass-balance simulation, the inflated inflow estimates falsely raise calculated reservoir storage and mask imminent deficits, shifting the release schedule toward aggressive early allocations for urban raw water and hydropower and leaving no buffer for the downstream Ciujung River. The resulting artificial drawdown pushes discharges below critical eco-flow thresholds during the April-September period (Simeone *et al.*, 2024), when the mandated 3.06 m^3/s environmental release is already below the Tennant (1976) "fair" threshold of 3.84 m^3/s (30% of MAF), creating conditions under which riparian ecosystems, macroinvertebrate habitats, and benthic communities would plausibly face elevated stress based on established eco-hydrological relationships; the present study did not directly

Table 2: Comparative statistical performance of ARIMA, MLR, and Markov chain inflow models for Karian reservoir

Metric	ARIMA	Markov Chain (3-class)	MLR
R (guideline vs actual trajectory)	0.76	0.80	0.85
Calibration (1998–2023) Correlation (r)	0.62	0.67	0.74
Calibration (1998–2023) KGE	0.60	0.66	0.64
RMSE (m^3/s)	4.97	4.69	4.08
MAE (m^3/s)	3.45	3.21	2.63
NSE	0.32	0.40	0.54
MAPE (%)	33.2	29.8	26.1

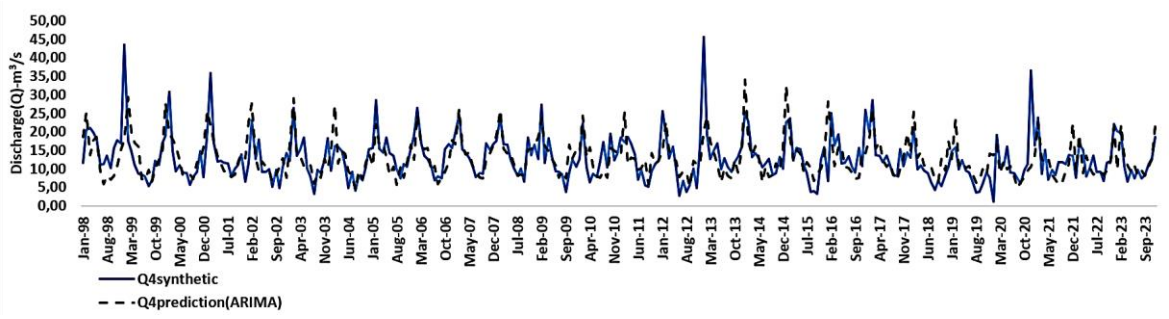

Fig. 2: Comparison of historical (Q4synthetic) and ARIMA-predicted monthly inflow discharge (1998-2023); the model systematically compresses wet-season peaks and overestimates dry-season baseflows, yielding the weakest fit among the three models (r = 0.62, KGE = 0.60, RMSE = 4.97 m^3/s)

measure these biological responses, so this inference remains a hypothesis for future ecological monitoring rather than an established outcome. Despite these forecasting limitations, the ARIMA framework preserves core utility for capturing seasonal autocorrelation structures and multi-year macro-scale trends pertinent to overarching infrastructural planning. Consistent with its weakest r and KGE, the ARIMA model also recorded the least favorable error metrics among the three frameworks (Table 2): RMSE = 4.97 m^3/s, MAE = 3.45 m^3/s, NSE = 0.32 (below the 0.5 satisfactory threshold of Moriasi *et al*. (2007), and MAPE = 33.2%. Despite this comparatively weaker point-to-point accuracy, a paired t-test (p = 0.937) and a Wilcoxon signed-rank test (p = 0.470) both failed to reject the null hypothesis of no systematic difference between ARIMA-simulated and historical inflow values, indicating that ARIMA's shortcomings manifest as reduced precision and event-scale responsiveness rather than a directional (systematic) bias.

Markov chain model performance

By shifting from a deterministic time-series architecture to a probabilistic formulation, the Markov Chain model facilitated a deeper comprehension of underlying state-transition dynamics. The stochastic model reached an event-scale correlation (r) of 0.67 and an aggregate KGE of 0.66 (Table 2). To observe how the probabilistic discretization translates into a continuous hydrograph trajectory, the chronological performance of the Markov Chain framework is displayed in Fig. 3. A particularly striking finding is the KGE statistical parity between the Markov Chain and the more responsive MLR model. Although constrained by lower event-scale correlation, the Markov Chain achieves comparable aggregate fidelity in replicating the long-term historical probability distribution of reservoir inflow, independently of localized, real-time hydrometeorological predictors. This capability stems from the model's underlying mathematical formulation.

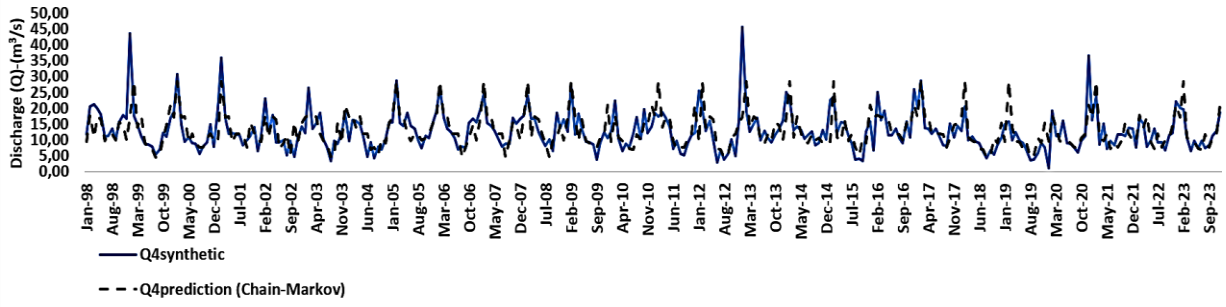

Fig. 3: Comparison of historical (Q4synthetic) and Markov Chain-predicted monthly inflow discharge (1998-2023); despite a lower event-scale correlation than MLR, the model closely reproduces the long-term probability distribution of historical inflow (r = 0.67, KGE = 0.66)

By discretizing the inflow hydrograph into three distinct probabilistic states and estimating the lag-1 Markovian transition matrix (Pij), water resource managers can quantify the probability of the system persisting in a 'dry' state across consecutive months. This framework effectively captures the temporal clustering of drought characteristic of the monsoonal tropics, where extended dry spells are driven by macroclimatic oscillations such as ENSO and the Indian Ocean Dipole (IOD) rather than isolated single-month fluctuations. Such prolonged dry spells are highly consequential, reducing available downstream discharge to the critical R10 threshold of just 1.22 m^3/s. The quantification of these transition probabilities provides a foundation for proactive "hedging rules". By executing gradual supply reductions at the onset of the dry season, systems can circumvent the need for sudden, reactive multi-sectoral allocation cuts near dead storage thresholds (Jehanzaib *et al.*, 2020; Yaseen *et al.*, 2018), ensuring the preservation of the 3.06 m^3/s environmental baseline during vulnerable low-flow window. In terms of point-accuracy error metrics (Table 2), the Markov Chain model achieved RMSE = 4.69 m^3/s, MAE = 3.21 m^3/s, NSE = 0.40, and MAPE = 29.8%, positioning it between ARIMA and MLR: an improvement over ARIMA across all four metrics, yet still below the 0.5 NSE threshold considered satisfactory by Moriasi *et al.* (2007). As with the other two models, a paired t-test (p = 0.518) and a Wilcoxon signed-rank test (p = 0.137) both failed to reject the null hypothesis of no systematic difference between Markov Chain-simulated and historical inflow values, confirming that the model's comparatively lower point-to-point precision does not reflect a systematic bias. Notwithstanding this positive cumulative performance, the Markov chain methodology entails specific methodological limitations necessitating careful consideration. First, the model's transition probabilities are entirely dependent on the historical record used to estimate them (1998-2018 in the calibration-only formulation reported above), and, as demonstrated by the independent validation results, these probabilities do not automatically adapt if the underlying climatic regime shifts. Second, the formulation relies on the premise of stationary, time-invariant state-transition probabilities, which could fail under the non-stationary environmental forcing—including intensified ENSO/IOD cycles and land-use modifications—underlying the broader scope of this retrospective analysis. Consequently, conducting formal tests of stationarity (such as transition-homogeneity or Markov-order diagnostics) is identified as a key direction for future work. Third, the model's three-state (dry/normal/wet) discretization operates at a coarser resolution than the continuous forecasts produced by ARIMA and MLR, trading event-scale precision for robustness in capturing long-term probabilistic drought patterns across dynamic, highly variable hydrological environments under changing climate conditions.

MLR model performance

Evaluation of the alternative approaches revealed that the MLR model attained the highest cumulative predictive accuracy and temporal sensitivity at the event scale. It achieved a correlation coefficient (r) of 0.74 and a KGE of 0.64 (Table 2). The temporal alignment and high precision of this deterministic baseline model across the historical 1998–2023 timeline are illustrated in Fig. 4. The correlation coefficient of r = 0.74, the highest among the three evaluated models, corroborates that a well-formulated multivariate linear structure captures the dominant rainfall-discharge teleconnections governing inflow variability at Karian, translating into accurate tracking of individual monthly high- and low-flow fluctuations with direct operational relevance for release scheduling and adaptive spillway management. This predictive robustness is anchored in the model's predictor combination, P1t-1 (Banjar Irigasi), P4t-1 (Sajira), and the lagged inflow Qin,t-1, of which the lagged inflow term is the dominant driver while the two rainfall stations contribute secondary, spatially-distributed information on upstream hydrological connectivity to the reservoir inlet (see robustness check below). Specifically, the lagged inflow term in particular functions as a mathematical proxy for the physical transit time between precipitation and downstream channel response, capturing the catchment's "memory". In steep tropical regimes, soil moisture dynamics operate as a natural low-pass filter that dampens high-frequency variability, ultimately dictating the translation of prior precipitation and baseflow recession into sustained runoff (Hasan *et al*., 2025; Wang *et al*., 2023). The high operational trajectory correlation (R = 0.85) achieved during the reservoir trajectory simulation confirms that MLR's linear formulation effectively approximates this physical lag-time behavior. In contrast to data-intensive machine learning algorithms that demand heavy computational overhead and rigorous long-term sensor calibration, this calibrated MLR structure offers water authorities a transparent, verifiable, and lightweight alternative for operational forecasting. The framework effectively links raw statistical inputs to monthly management schedules, allowing reservoir operations and sectoral water distribution to be governed by mechanistic catchment moisture trends instead of generalized statistical norms. The additional error metrics computed for MLR corroborate its superior performance (Table 2): RMSE = 4.08 m^3/s and MAE = 2.63 m^3/s were the lowest among the three models, NSE = 0.54 was the only value exceeding the 0.5 satisfactory threshold of Moriasi *et al.* (2007), and MAPE = 26.1% was likewise the lowest. A paired t-test (p = 0.923) and a Wilcoxon signed-rank test (p = 0.757) both failed to reject the null hypothesis of no systematic difference between MLR-simulated and historical inflow values, indicating that MLR combines the best point-accuracy performance among the three models with an absence of systematic bias over the 1998-2023 calibration period. To ascertain whether the observed point-estimate divergences among the three models remain resilient against sampling variability, 95% confidence intervals were generated using a moving block bootstrap approach (B = 2,000; utilizing 12-month blocks). MLR's advantage in MAE was robust specifically against ARIMA, and its NSE advantage over ARIMA was likewise robust, as the respective 95% CIs did not overlap (MLR MAE: 2.33-2.98 m^3/s vs ARIMA: 3.05-3.90 m^3/s; MLR NSE: 0.46-0.64 vs ARIMA: 0.20-0.44); MLR's MAE advantage over Markov Chain (2.94-3.55 m^3/s) was not statistically robust, as the two 95% CIs overlapped narrowly. However, the 95% CIs for r, KGE, RMSE, and MAPE overlapped substantially across all three models, meaning that the apparent ranking on these metrics falls within the bounds of sampling uncertainty given the 26-year monthly record and should not be over-interpreted as a robust, generalizable difference. Consequently, the MLR model is best interpreted as yielding the most competitive point estimates across all evaluated metrics—demonstrating a statistically robust advantage over ARIMA specifically in terms of

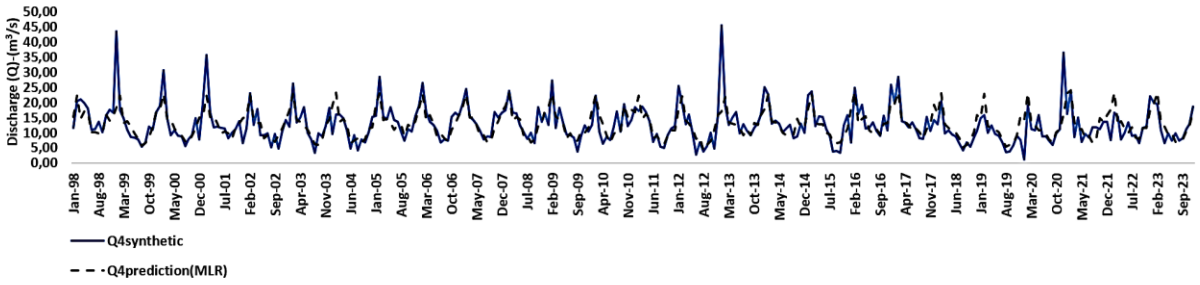

Fig. 4: Comparison of historical (Q4synthetic) and MLR-predicted monthly inflow discharge (1998-2023), showing the closest event-scale tracking among the three models (r = 0.74, KGE = 0.64, RMSE = 4.08 m^3/s), driven primarily by the lagged-inflow predictor

mean absolute error and NSE—rather than exhibiting uniform superiority across every performance dimension. As detailed in Materials and Methods, the twelve month-specific MLR models (Eq. 1) that together generate the calibration series evaluated in Table 2 each rely on a comparatively small per-month sample (n = 26-27 years). Examining the coefficients of these twelve models individually shows that the lagged inflow term (Qin,t-1) is by far the most consistently significant predictor ($p < 0.05$ in 7 of 12 months, concentrated in the May-November transition and dry-season months), whereas P4,t-1 (Sajira) is significant in only one month and P1,t-1 (Banjar Irigasi) is not statistically significant in any month; variance inflation factors remained below 2 throughout, indicating that this pattern reflects genuine predictor importance rather than multicollinearity, and confirming that MLR's predictive skill is driven primarily by the catchment-memory mechanism encoded in Qin,t-1, with the upstream rainfall stations contributing secondary, spatially-distributed information. Leave-one-out cross-validation of these twelve month-specific models shows negative out-of-sample R2 in 6 of 12 months (mean overfitting gap = 0.30), indicating that, taken individually, several of the month-specific models are statistically fragile at this sample size. This trade-off is evaluated against the considerably enhanced overall goodness-of-fit afforded by monthly stratification relative to a pooled-coefficient configuration (r = 0.40, NSE = 0.16; as stated in Materials and Methods section), a convention conceptually analogous to the seasonal parameterization already incorporated into the comparative ARIMA and Markov Chain formulations. Reported MLR performance in Table 2 should therefore be interpreted as the aggregate behavior of twelve seasonally-specific models rather than of a single model generalizing across a large, homogeneous 312-month sample, and the per-month overfitting risk identified here is noted as a limitation in the Study limitations section. Beyond the sample-size and seasonal stratification issues previously addressed, a further structural drawback inherent to the MLR architecture is its rigid linear formulation. Rainfall-runoff mechanisms within steep tropical basins are characterized by distinct threshold-dependent non-linearities. These include storm flow activation governed by antecedent soil moisture saturation limits, as well as non-linear infiltration and groundwater recession behaviors that exceed the representational capacity of conventional linear modeling architecture. This is a plausible contributing explanation for MLR's own moderate (not outstanding) r and KGE values (Table 2) and for the sharp performance degradation observed under independent out-of-sample validation (see above), since nonlinear catchment behavior that differs between the calibration and validation periods cannot be captured by a fixed linear coefficient set. Future work extending this comparison to nonlinear or hybrid statistical models (e.g., ARIMA-LSTM, as noted in the

Outlook) would help isolate how much of the observed performance gap is attributable to linearity itself versus non-stationarity. To explicitly evaluate the independence between the calibration and validation samples, all three modeling frameworks—ARIMA, MLR, and the Markov chain—were further subjected to a strict chronological train-test split. For both the MLR and Markov Chain, state classification thresholds, transition probabilities, and the twelve month-specific regression coefficients (Eq. 1) were derived exclusively from the 1998-2018 dataset. These calibration-derived parameters were subsequently applied without modification or re-fitting to the independent 2019-2023 evaluation period. For ARIMA, the model order was independently re-identified via automated seasonal ARIMA selection on a training subset (n=263) rather than applied from the full-record specification reported in Table 2, yielding ARIMA(1,0,0)(1,1,0)[12] with drift, distinct from the full-record SARIMA(2,0,1)(2,1,2)[12] model; this training/testing split (n=263/61) operates on the undifferenced 1997-2023 series required for ARIMA's seasonal differencing and consequently begins approximately one month earlier than the calendar-aligned 1998-2018/2019-2023 split used for MLR and Markov Chain, though the two splits are closely comparable in both timing and proportion (81%/19% versus 81%/19%). Aggregate performance across all three models and both periods is summarized in Table 3. Although predictive performance declines across the independent validation dataset for all three modeling frameworks, the extent of degradation varies substantially among them. For MLR, NSE falls from 0.61 (calibration) to 0.02 (validation), a value indistinguishable from a naive mean predictor, and MAPE more than doubles from 21.9% to 50.2%. In contrast, the Markov Chain model exhibits an even more pronounced degradation: its state-classification thresholds, transition probabilities, and state-conditional mean discharges, all parameterized exclusively on the 1998-2018 data, achieve NSE = 0.28 in calibration but fall to NSE = -1.01 in validation. This indicates that the calibration-derived model performs worse than utilizing the simple historical mean for the 2019–2023 evaluation period, accompanied by an increase in MAPE from 30.8% to 81.6%. ARIMA, by contrast, shows comparatively modest degradation: NSE falls only from 0.37 (training) to 0.29 (testing), and its correlation coefficient decreases only slightly, from 0.66 to 0.60, despite ARIMA having the lowest calibration-period accuracy of the three models in Table 2. This divergent behavioral pattern provides key insights: the purely autoregressive, seasonally differenced structure of the ARIMA model does not depend on exogenous rainfall or lagged-inflow predictors whose relationship to Qin may itself be shifting, which plausibly makes it less sensitive to the specific form of non-stationarity affecting the exogenous-predictor-dependent MLR and state-transition-dependent Markov Chain models, even though this parsimonious structure simultaneously limits its overall absolute predictive accuracy. This degradation was not an artifact of the particular split year chosen for MLR: repeating the same procedure at six additional split points boundaries spanning 2012-2021 consistently yielded near-zero or negative validation NSE (range: -0.22 to 0.07), irrespective of where the calibration-validation threshold was established. Rather than weakening the central hypothesis, this phenomenon—most pronounced in the Markov chain simulations and observable even within ARIMA's minor degradation—reinforces the fundamental premise of this investigation. Specifically, models calibrated against past hydrological regimes cannot be presumed transferable to future periods in the presence of a non-stationary precipitation-discharge dynamic, regardless of whether the underlying architecture is regression-based, stochastic, or autoregressive. This underscores the necessity for continuous retrospective appraisal of design-era assumptions in lieu of their indefinite operational reuse. The calibration-only

Table 3: MLR, Markov Chain and ARIMA performance under chronological calibration (1998-2018) versus independent out-of-sample validation (2019-2023)

Metric	MLR calibration (1998-2018, n=252)	MLR validation (2019-2023, n=60)	Markov Chain calibration (1998-2018, n=252)	Markov Chain validation (2019-2023, n=60)	ARIMA training (n=263)	ARIMA Testing (n=61)
r (Pearson correlation)	0.78	0.56	0.66	0.32	0.66	0.60
RMSE (m^3/s)	3.85	5.48	5.19	7.86	4.92	4.64
MAE (m^3/s)	2.48	3.65	3.45	5.35	3.41	3.34
NSE	0.61	0.02	0.28	-1.01	0.37	0.29
MAPE (%)	21.9	50.2	30.8	81.6	29.6	47.3

performance reported in Table 2 (MLR: r = 0.74, NSE = 0.54; Markov Chain: r = 0.67, KGE = 0.66; ARIMA: r = 0.62, KGE = 0.60; all computed by fitting and evaluating on the full 1998-2023 record) should accordingly be interpreted as an upper-bound estimate of in-sample fit quality rather than a guarantee of forecasting skill on unseen future periods.

Hydrological year classification and operation guideline trajectories

To bridge the inflow forecast with practical field enforcement, a non-parametric frequency analysis was performed. In lieu of alternative return-period estimators (such as the Gumbel, Log-Pearson III, and California/Hazen formulations), the Weibull plotting-position method was adopted. This approach is favored due to its unbiased nature and prominent status in Indonesian hydrological practice for dependability and return-period assessment. Crucially, unlike parametric distribution-fitting approaches (e.g., Log-Pearson III), it dispenses with a-priori assumptions regarding the parent probability distribution of monthly inflow, thereby mitigating uncertainties stemming from the catchment's limited 26-year instrumental record. Weibull probability analysis applied to the multi-decade dataset yielded reliable discharge thresholds of 9.51 m^3/s (P80% or R5 dry, representing dry year conditions), 15.65 m^3/s (P50% or R2 normal, representing normal year conditions), and 21.66 m^3/s (P20% or R5 Wet, representing wet year conditions). The full seasonal variation of these reliable flows across the various reliability classes is structurally illustrated in Fig. 5. The R5 discharge limit was adopted as the primary basis for Phase 1 water allocation, allocating 6.45 m^3/s for the Tangerang raw water covered tunnel and a nominal 3.06 m^3/s for the downstream flow of the Ciujung River. Crucially, the R5-estimated discharge surpasses the baseline operational threshold of 2.20 m^3/s previously stipulated by the regional water authority (BBWS C3 2025) with an incremental addition of 0.86 m^3/s, thereby yielding a 39.09% upward adjustment. This adjustment closes approximately 47.78% of the operational gap towards the ideal design drought discharge reference of 4.0 m^3/s required for full ecosystem preservation (KOICA, 2006), with a remaining gap of 0.94 m^3/s remaining unmet. However, under severe R_{10} hydrological constraints, the residual streamflow entering the Ciujung River sharply declines to 1.22 m^3/s. Such streamflow volumes fall critically short of the thresholds required to operate the 1.8 megawatt (MW) run-of-river hydropower turbines and maintain downstream aquatic ecosystem integrity, underscoring the severe ecological susceptibility of the catchment. To systematically manage these risks, long-term operation guideline trajectories were derived using the Rippl Method mass-balance reservoir simulation. The resulting monthly volume trajectories for each hydrological year class are detailed in Fig. 6. As depicted in Fig. 6, reservoir storage behavior exhibits highly seasonal and monsoon-dependent characteristics. Active storage begins at a relatively low level in January, with wet-year volumes starting at approximately 39.55 million m^3, normal-year volumes at 20.14 million m^3, and dry-year volumes at 6.46 million m^3.

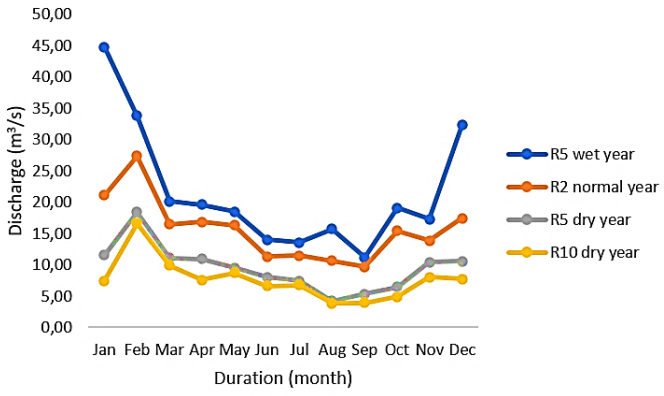

Fig. 5: Monthly distribution of Karian Reservoir dependable discharges across four Weibull reliability classes (R_5 wet year to R_{10} dry year), showing the sharp dry-season contraction from the R5 Dry threshold of 9.51 m^3/s to a residual R10 discharge of just 1.22 m^3/s

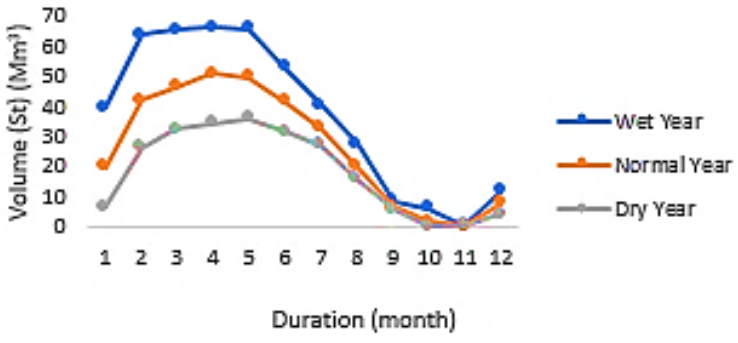

Fig. 6: Three-class operation guideline trajectory curves for Karian Reservoir (dry, normal, and wet year classifications) derived from the Rippl mass-balance simulation, showing active storage accumulating to a wet-year peak of 66.42 million m3 in April before contracting to near-zero levels during the September-November low-flow period

Active storage volumes exhibit a progressive accumulation phase throughout the monsoon, reaching absolute peak capacity in April for both wet-year (66.42 million m^3) and normal-year (50.86 million m^3) conditions, while peaking slightly later in May (36.07 million m^3) in dry-year conditions. In contrast, water storage volumes exhibit a severe depletion phase beginning in June, driven by the steep decline in basin inflows characteristic of the dominant dry monsoon pattern. This downward trend culminates in near-zero active storage volumes during the critical September–November period, with storage reaching absolute zero in October (dry conditions) and November (wet and normal conditions). This interval of extreme low storage manifests as an annual bottleneck of ecological vulnerability, marked by the potential collapse of required downstream environmental flows within the critical Ciujung River reach. In accordance with established hydrodynamic and ecological principles observed in similar systems, such near-zero storage states would theoretically intensify vulnerability to localized saltwater encroachment in the estuary and associated habitat impacts, notwithstanding the omission of direct salinity and biodiversity measurements in the current study (Bauer *et al*., 2025).

Reservoir operation simulation

To evaluate how inflow forecasting errors propagate into long-term infrastructure behavior, the three generated inflow time series were integrated as direct forcing vectors into reservoir operation simulations. Model trajectories generated under the ARIMA, Markov chain, and

MLR frameworks are presented in comparative alignment across Figs. 7, 8, and 9. The ARIMA-forced simulation (Fig. 7) achieved a guideline-to-actual trajectory correlation (R) of 0.76. During the 1998–2005 wet seasons, actual simulated storage trajectories frequently exceeded target guideline envelopes due to the underestimation of high-flow periods by the ARIMA model. This indicates a high risk of uncontrolled spillway losses and unutilized hydro-potential. The probabilistic Markov chain simulation (Fig. 8) achieved an improved R of 0.8, displaying more consistent trajectory tracking and tighter adherence to the target boundary conditions across both average and wet sequences. The MLR-forced simulation (Fig. 9) achieved superior predictive capability with a correlation coefficient of R = 0.85, establishing a stable discharge regime while effectively mitigating large excursions from target guidelines. This outcome provides empirical evidence favoring the operational use of MLR-based inflow scenarios for long-term planning, with the caveat noted above that this advantage is statistically robust for MAE and NSE but not yet distinguishable from sampling uncertainty for r, KGE, RMSE, and MAPE. Crucially, while keeping all internal operational boundary constraints fixed, all three models mathematically confirm that the Karian Reservoir possesses adequate structural capacity to satisfy Phase 1 mandatory multi-sectoral release obligations under standard climatological conditions. However, the MLR framework minimizes risk by preventing abrupt over-releases.

Eco-hydrological trade-offs and multi-sectoral allocation dynamics

Integrating these forecasting structures into the multi-objective water balance equation illuminates the severe operational trade-offs inherent to the Karian Reservoir system under hydrological constraints. Severe inflow reductions reaching extreme dry-year thresholds (R10) diminish the residual operational margin to negligible levels, thereby intensifying the trade-off between human water infrastructure requirements and downstream aquatic ecological survival (Poff *et al*., 2010; Arthington *et al*., 2024). This convergence between infrastructure operation and river ecosystem service provision underscores the value of coupling landscape-scale ecological assessments with reservoir release planning (Dede *et al*., 2023). Total reservoir discharge is routed through two distinct, physically segregated conduits. A closed tunnel supplies the fixed-priority, legally non-negotiable urban raw water withdrawal for Tangerang, whose design allocation evolved from an original 9.1 m^3/s to 12.4 m^3/s before settling at the current Phase 1 value of 6.45 m^3/s. An open channel, feasibility-study design capacity 5.5 m^3/s, first routes water through the 1.8 MW run-of-river hydroelectric power plant turbines before releasing the same water to the Ciujung/Ciberang system to jointly serve raw water supply, irrigation, and river-maintenance (environmental) flow; the feasibility study did not subdivide this 5.5 m^3/s into separate, individually protected sub-allocations for each use; it estimated a combined river-maintenance requirement of approximately 4.0 m^3/s but did not wall this off as a reserved quantity within the 5.5 m^3/s design total. Crucially, the prevailing rule structure fails to treat environmental flow as an adaptive constraint capable of dynamically adjusting releases during low-storage events. Throughout this study, the frequently referenced 3.06 m^3/s environmental flow figure is more accurately defined as the total open-channel residual under R5 dry-year dependable-flow conditions. Specifically, this figure represents the 9.51 m3/s total inflow minus the 6.45 m^3/s tunnel withdrawal, which is shared among raw water supply, irrigation, and river maintenance. As raw water and irrigation draws draw from this shared pool, actual water availability for ecological integrity is heavily constrained. Consequently, the ecological-risk assessments evaluated against Tennant thresholds serve as conservative, upper-bound estimates of e-flow stress rather than exact measurements of dedicated environmental allocations (BBWS C3, 2025) allocates the Karian-side intake serving the Serang area as 1.5 m^3/s raw

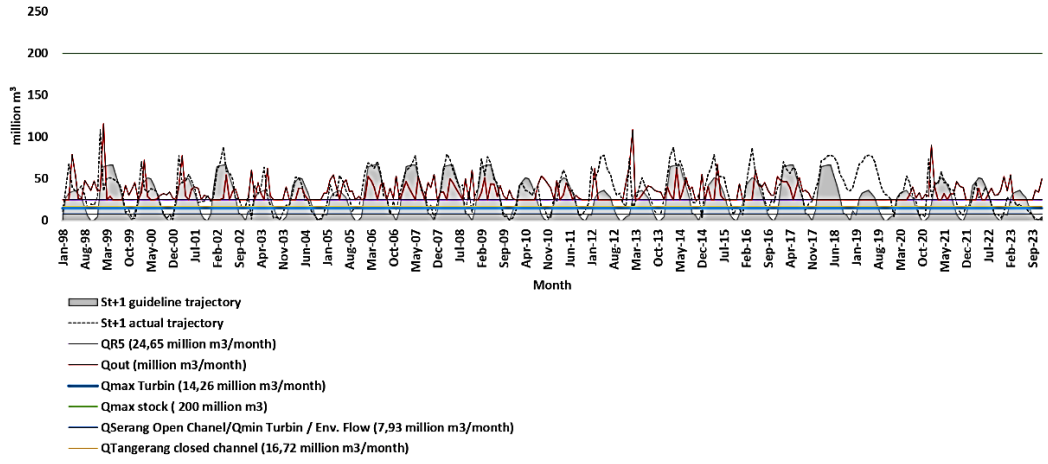

Fig. 7: ARIMA-based reservoir operation simulation showing St+1 guideline and actual trajectories with operational parameters (1998–2023); actual storage frequently overshoots the guideline envelope during 1998-2005 wet seasons (R = 0.76), indicating a risk of uncontrolled spillway losses

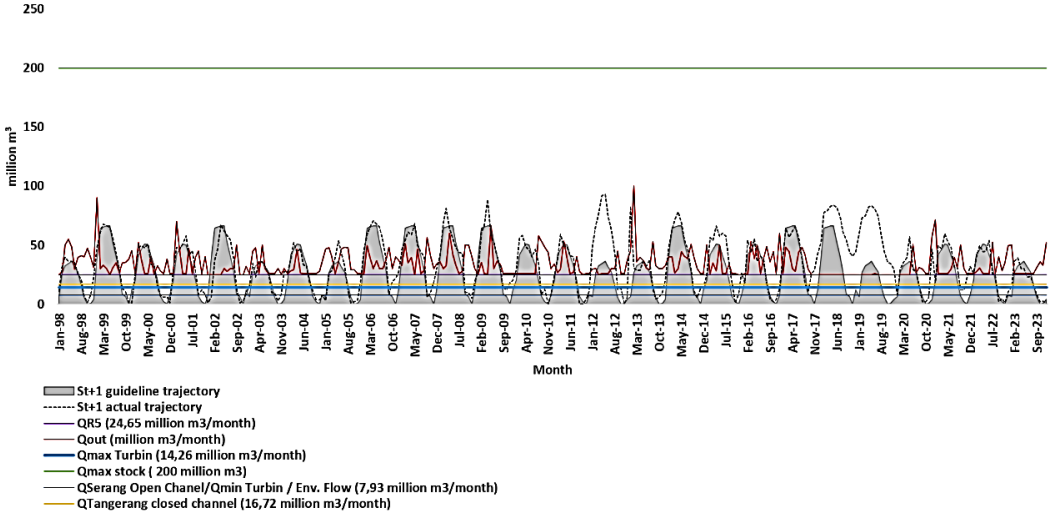

Fig. 8: Markov chain-based reservoir operation simulation showing St+1 guideline and actual trajectories with operational parameters (1998–2023), displaying more consistent trajectory tracking than ARIMA (R = 0.80) across both average and wet sequences

water supply plus 0.7 m^3/s irrigation (2.2 m^3/s total), without an explicit environmental-flow or hydropower line item comparable to the original feasibility study's provisions; whether this reflects an actual removal of environmental-flow consideration from current operational planning, or simply its omission from this particular planning summary while it is retained in other unpublished technical documents, could not be determined from the materials available to this study and is noted here as an area requiring clarification with the implementing agency rather than as an established finding. The performance of operational simulations reveals significant vulnerabilities when utilizing uncoupled or systematically biased models like ARIMA. Specifically, under R10 conditions, these predictive inaccuracies force the designated 3.06 m^3/s environmental flow down to a deficient minimum of 1.22 m^3/s. This extreme truncation would be expected to severely diminish the river's ecological assimilative capacity; based on

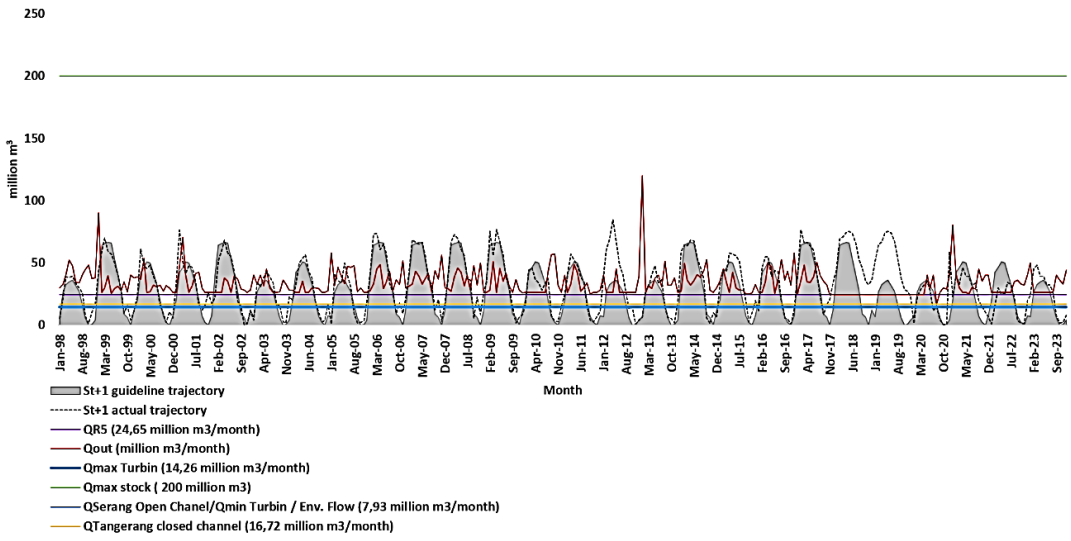

Fig. 9: MLR-based reservoir operation simulation showing St+1 guideline and actual trajectories with operational parameters (1998–2023); the closest adherence to the guideline envelope among the three models (R = 0.85) yields the most stable, risk-minimizing discharge pattern

mechanisms documented in comparable low-flow systems, such conditions could plausibly contribute to dissolved oxygen depletion and saltwater estuarine intrusion upstream, although these water-quality and salinity responses were not directly measured in the present study (Wu *et al.*, 2023). As previously noted, the R5-derived allocation narrows the historical design gap by approximately 39.09% relative to the minimum threshold recommended by the regional authority. Despite this improvement, a deficit of 0.94 m^3/s remains against the complete ecosystem-preservation objective (KOICA, 2006). Conversely, by deploying the complementary MLR-Markov Chain decision-support architecture proposed in this study, reservoir operators can balance these trade-offs dynamically (Li and Zhu, 2025). This methodological framework must comprehensively address multiple socio-environmental dimensions. Crucially, it needs to balance social legitimacy and water-quality trade-offs among the local communities dependent on the shared reservoir (Al-Afeshat *et al.*, 2025). The MLR provides the short-term precision needed to maximize run-of-river hydropower generation during transient wet intervals (Yajure-Ramírez, 2026), while the Markov chain framework provides the long-term probabilistic warning required to trigger ecological water rationing, preventing the complete collapse of downstream riparian eco-services during macroclimatic anomalies (Huang *et al.*, 2026).

Outlook for advancing sustainable reservoir management

This comparative study highlights that while the deterministic MLR model excels as an operational tool for creating guideline trajectories (R = 0.85, r = 0.74, KGE = 0.64), the Markov Chain model acts as a vital probabilistic instrument to safeguard against severe drought risks. Incorporating this complementary MLR-Markov Chain approach offers a low-cost, practically implementable decision-support approach that accounts for hydrological environmental-flow thresholds, rather than a validated ecologically sensitive system, since ecological outcomes were not directly evaluated in this study (see Study limitations). This framework can guide water authorities in simultaneously balancing all five competing Phase 1 strategic mandates at the Karian Reservoir. A primary limitation of this study is its reliance on the reconstructed Q_{in} synthetic inflow record. Nevertheless, this framework exhibits inherent limitations under conditions of hydrological non-stationarity. Such regime

shifts—stemming from anthropogenic climate change, intensive land-use alterations, and amplified ENSO/IOD teleconnections across the Indonesian archipelago—pose ongoing challenges to long-term projections (Irwandi *et al*., 2021). To advance sustainable reservoir management in tropical monsoonal zones, future research should prioritize three key domains:

- Development of hybrid ARIMA-LSTM (long short-term memory) networks and gradient boosting machines to better map non-stationary, non-linear peak discharge variations (Kratzert *et al*., 2019).
- Integration of downscaled CMIP6 climate change projections and dynamic land-use conversion scenarios directly into the water balance equation.
- To build regional resilience against extreme climate anomalies, this comparative eco-hydrological evaluation framework warrants systematic replication. Specifically, its application should be extended to other strategic, multipurpose tropical reservoirs throughout Southeast Asia.

The empirical evidence established through this multi-model framework demonstrates that transitioning from traditional linear approaches to a complementary MLR-Markov chain paradigm provides a robust, data-driven foundation for tropical reservoir management worldwide. Crucially, the MLR and Markov Chain components were formulated, calibrated, and validated as independent frameworks within this study, omitting any joint calibration or optimized structural coupling. The framing of these models as 'complementary' is therefore strictly conceptual. It denotes their separate operational roles in short-term guideline generation versus long-term drought-risk screening, rather than an interconnected modeling architecture. By accurately capturing seasonal inflow variations and quantifying drought state-transition probabilities, this two-model approach offers a transferable framework that may inform operation planning at other tropical monsoonal reservoirs facing similar trade-offs between hydropower generation and downstream environmental flow protection, pending validation across additional basins and climate scenarios.

Study limitations and future directions

Several methodological limitations of this study warrant consideration. First, eco-flow compliance was evaluated strictly using hydrological proxy thresholds (specifically the Tennant method) rather than direct *in situ* biological sampling. Qualitative inferences regarding ecological risk—such as dissolved oxygen depletion or benthic habitat stress, are fundamentally anchored to minimum volumetric discharge thresholds established for aquatic habitat preservation. They do not stem from direct empirical observations of biological responses. Future research should integrate multi-seasonal biological monitoring with hydrodynamic modeling to empirically validate ecological outcomes under simulated release strategies. Second, because the Karian Reservoir lacks an operational inlet gauging station, the reconstructed inflow (Qin) baseline cannot be independently validated through on-site measurements. While internal consistency with legacy estimates (KOICA area-ratio) was verified, both approaches rely on the same downstream reference station (Q7), representing an inherent monitoring constraint to be prioritized in future instrumentation efforts. Third, the predictive performance obtained here ($r = 0.62–0.75$, KGE = 0.60–0.66) is more conservative than metrics reported in longer-record tropical reservoir studies. For instance, comparative applications of Markov Chain, NRECA, ARIMA, and continuous models at Jatigede Reservoir, Indonesia achieved substantially higher accuracy (Jayanti *et al*., 2023), while MLR, ARIMA, and SARIMA models at Koyna Reservoir, India (Magar and Jothiprakash, 2011) and across East Java reservoirs (Margini *et al*., 2022) also demonstrated strong predictive performance. These regional discrepancies do not stem from any methodological shortcoming. Instead, they reflect Karian's shorter 26-year record, the retention of extreme events, and dynamic monsoonal

variability. Moreover, fitting month-specific MLR models on 26–27 years of data introduces sampling uncertainty, leading to variable out-of-sample generalization despite outperforming a single pooled formulation. Subsequent studies should evaluate alternative modeling strategies, including harmonic regression and partial pooling. Incorporating these frameworks will help capture finer seasonal dynamics while optimizing sample efficiency. Finally, because all models were calibrated for a single monsoonal catchment (Karian/Ciberang), extending this framework to catchments with distinct hydroclimatic regimes (such as snowmelt influence or bimodal rainfall) will require structural adjustments and independent re-validation.

CONCLUSION

This study evaluated three low-data statistical inflow forecasting frameworks—MLR, Markov Chain, and ARIMA—against the Karian Reservoir's historical hydrological record (1998–2023) to examine whether design-era operational assumptions remain hydrologically defensible under present-day flow regimes. The historical calibration period (1998–2018) revealed considerable variation in functional performance characteristics across the evaluated methodologies. MLR achieved the highest calibration accuracy ($r = 0.74$, KGE = 0.64, $R = 0.85$) by effectively leveraging lagged inflow variables to capture catchment storage memory and temporal persistence. While delivering a comparable overall efficiency (KGE = 0.66), the Markov Chain framework excelled in capturing complex hydrological patterns. Specifically, it exhibited enhanced capability in reproducing long-term probability distributions and structural low-flow characteristics. Conversely, ARIMA produced the weakest baseline performance ($r = 0.62$, KGE = 0.60), largely driven by a systematic overestimation of dry-season baseflow. This constraint reveals a fundamental structural limitation of the ARIMA model. Specifically, it lacks the technical capacity to accommodate extreme seasonal fluctuations without introducing substantial signal distortion in monsoonal hydrological systems. Critically, independent out-of-sample validation (2019–2023) revealed a severe performance degradation across all frameworks. The NSE for MLR plummeted from 0.61 to 0.02, while the Markov Chain framework dropped drastically from 0.28 to -1.01. The marked degradation in predictive capability confirms the presence of hydrological non-stationarity across the catchment. This degradation demonstrates that traditional models parameterized on past hydroclimatic regimes require continuous adaptive recalibration to maintain long-term reliability. Consequently, these empirical findings directly address the primary objective of this study: no single low-data statistical model evaluated here is dependably robust for static operational deployment over long horizons. Furthermore, the original design-era environmental-flow target of 3.06 m^3/s must be re-categorized as provisional. Adhering to inflexible historical release rules compromises downstream aquatic ecosystems and water-supply security. As runoff patterns deviate increasingly from stationary historical baselines, these systems face compounded operational vulnerabilities. The broader scientific and practical implications of these findings highlight the urgent need to transition from deterministic, static reservoir operating policies toward dynamic, risk-based operational strategies in data-scarce tropical basins. Relying solely on historical statistical relationships creates a false sense of operational security, particularly during prolonged dry spells or extreme convective rainfall events. By illustrating the performance decay of conventional statistical models under non-stationary hydroclimatic regimes, this work highlights a critical operational requirement. Specifically, it emphasizes the imperative to incorporate real-time feedback mechanisms into modern reservoir management frameworks. Adaptive management protocols must replace legacy operational rules to reconcile competing demands between municipal water supply, flood control, and downstream ecological integrity.

These findings should, however, be interpreted with due consideration of specific methodological constraints. First, the analysis relied on a single reconstructed catchment inflow dataset, which may carry unresolved observational uncertainties or spatial aggregation biases from streamflow routing approximations. Second, rather than utilizing direct in-situ biological sampling of fish or macroinvertebrate communities, ecological adequacy was assessed via hydrological proxy indicators. Specifically, this study adopted the Tennant methodology to establish environmental flow requirements. Third, because calibration was restricted to a single reservoir catchment, specific numerical parameters and degradation rates observed here may not transfer to other climatic zones or topographically diverse catchments without independent local revalidation.

AUTHOR CONTRIBUTIONS

I. Mulyawati, prepared in data curation, formal analysis, investigation, visualization and preparing the manuscript draft. I.R.S. Salami, the first promotor and corresponding author, supervised the first author, contributed to conceptualization, and reviewed the manuscript. M. Marselina, the second promotor, also supervised the first author and contributed to conceptualization and manuscript review. A. Sabar, the third promotor, supervised the first author, contributed to conceptualization, and reviewed the manuscript.

ACKNOWLEDGEMENT

I. Mulyawati was supported by the Center for Higher Education Funding and Assessment (PPAPT), Ministry of Higher Education, Science, and Technology of the Republic of Indonesia, and the Indonesia Endowment Fund for Education (LPDP), Ministry of Finance of the Republic of Indonesia, through the Beasiswa Pendidikan Indonesia (BPI) for doctoral studies [Grant number: 202101121537]. The authors gratefully acknowledge BBWS C3, Banten Province, Indonesia, for providing hydrological monitoring network data and the location map of Karian Reservoir during a series of field visits conducted between 2021 and 2025.

CONFLICT OF INTEREST

The authors declare that there is no conflict of interests regarding the publication of this manuscript. In addition, the ethical issues, including plagiarism, informed consent, misconduct, data fabrication and/or falsification, double publication and/or submission, and redundancy have been completely observed by the authors.

OPEN ACCESS

©2027 The author(s). This article is licensed under a Creative Commons Attribution 4.0 International License, which permits use, sharing, adaptation, distribution and reproduction in any medium or format, as long as you give appropriate credit to the original author(s) and the source, provide a link to the Creative Commons license, and indicate if changes were made. The images or other third-party material in this article are included in the article's Creative Commons license, unless indicated otherwise in a credit line to the material. If material is not included in the article's Creative Commons license and your intended use is not permitted by statutory regulation or exceeds the permitted use, you will need to obtain permission directly from the copyright holder. To view a copy of this license, visit: http://creativecommons.org/licenses/by/4.0/

PUBLISHER'S NOTE

GJESM Publisher remains neutral with regard to jurisdictional claims in published maps and institutional affiliations.

POSITIVE AI STATEMENT

During the preparation of this work the author(s) have used Artificial Intelligence (AI) [Quillbot] in order to improve English language clarity, grammar accuracy, and academic phrasing of the manuscript. After using this tool/service, the authors reviewed and edited the content as needed and take full responsibility for the content of the publication.

ABBREVIATIONS

%	Percent
ACF	Autocorrelation function
AIC	Akaike information criterion
ARIMA	Autoregressive integrated moving average
BBWS C3	Balai Besar Wilayah Sungai Cidanau-Ciujung-Cidurian
BPI	Beasiswa Pendidikan Indonesia
CMIP6	Coupled Model Intercomparison Project Phase 6
DPI	Dots per inch
ENSO	El Niño-Southern Oscillation
FDC	Flow duration curve
IID	Independent-and-identically-distributed
IOD	Indian Ocean Dipole
KGE	Kling-Gupta efficiency
KOICA	Korea International Cooperation Agency
LPDP	Lembaga Pengelola Dana Pendidikan (Indonesia Endowment Fund for Education)
LSTM	Long short-term memory
MAF	Mean annual flow
m^3/s	Cubic meter per second
MLR	Multiple linear regression
MW	Megawatt
n	Sample size / number of time steps
NSE	Nash-sutcliffe efficiency
PPAPT	Pusat Pembiayaan dan Asesmen Pendidikan Tinggi (Center for Higher Education Funding and Assessment)
r	Pearson correlation coefficient
R	Operational trajectory correlation coefficient

REFERENCES

Aksoy, H., (2003). Markov chain-based modeling techniques for stochastic generation of daily intermittent streamflows. Adv. Water Resour., 26(6): 663–671 (**9 pages**).

Al-Afeshat, A.; Zoubi, M.M.; Abu-Afifeh, Q.Y.; Al-Jawaldeh, H.; Qutishat, T.A.; Masoud, A.M.N.; Rahbeh, M., (2025). Interrelation of dams sustainability with the local communities and water quality. Global J. Environ. Sci. Manage., 11(1): 157–176 (**20 pages**).

Aldrian, E.; Dwi Susanto, R., (2003). Identification of three dominant rainfall regions within Indonesia and their relationship to sea surface temperature. Int. J. Climatol., 23(12): 1435–1452 (**18 pages**).

Arianti, D.; Murtilaksono, K.; Barus, B., (2015). Evaluation of land use for design flood discharge prediction in Ciberang watershed, Banten Province. TATALOKA, 17(2): 76–86 **(11 pages).**

Arwin; Bourqueil, M., (1992). Modelisation des ressources en eau et leur exploitation énergétique sur l'exemple du bassin supérieur de Citarum en Indonesie. Doctoral Thesis. Toulouse, INPT (**250 pages**).

Alrayess, H.; Zeybekoglu, U.; Ulke, A., (2017). Different design techniques in determining reservoir capacity. Eur. Water, 60: 107–115 (**9 pages**).

Anand, V.; Oinam, B., (2019). Future climate change impact on hydrological regime of river basin using SWAT model. Global J. Environ. Sci. Manage., 5(4): 471–484 (**14 pages**).

Aness, W.Th.; Hadadin, N.A.; Zoubi, M.M.; Abu-Afifeh, Q.Y.; Al-Afeshat, A.F.; Al-Jawaldeh, H.F.; Qutishat, T.A.; AlHalaigah, M.R.; Alnizami, N.H.; Aljarrah, A.; Alta'any, Y.A.; Alzubaidi, A.J., (2026). Runoff and sediment dynamics modeling for erosion risk reduction and sustainable watershed management. Global J. Environ. Sci. Manage., 12(2): 813–836 (**24 pages**).

Arthington, A.H.; Tickner, D.; McClain, M.E.; Acreman, M.C.; Anderson, E.P.; Babu, S.; Dickens, C.W.S.; Horne, A.C.; Kaushal, N.; Monk, W.A.; O'Brien, G.C.; Olden, J.D.; Opperman, J.J.; Owusu, A.G.; Poff, N.L.; Richter, B.D.; Salinas-Rodríguez, S.A.; Shamboko Mbale, B.; Tharme, R.E.; Yarnell, S.M., (2024). Accelerating environmental flow implementation to bend the curve of global freshwater biodiversity loss. Environ. Rev., 32(3): 387–413 (**27 pages**).

Atieh, M.; Taylor, G.; Sattar, A.M.A.; Gharabaghi, B., (2017). Prediction of flow duration curves for ungauged basins. J. Hydrol., 545: 383–394 (**12 pages**).

Balai Besar Wilayah Sungai Cidanau-Ciujung-Cidurian (BBWSC3), (2025). Spatial data of Karian Reservoir watershed. Unpublished technical dataset, Ministry of Public Works and Housing, Banten, Indonesia.

Bargam, B.; Boudhar, A.; Kinnard, C.; Bouamri, H.; Nifa, K.; Chehbouni, A., (2024). Evaluation of the support vector regression (SVR) and the random forest (RF) models accuracy for streamflow prediction under a data-scarce basin in Morocco. Discov. Appl. Sci., 6: 306 (**18 pages**).

Bauer, J.; Dörr, F.; Vu, H.T.D.; Schenk, A.; Tran, H.V.; Pham, V.C.; Börsig, N.; van der Linden, R.; Nguyen, N.H.; Eiche, E.; Norra, S., (2025). Seawater intrusion in river delta systems. Inter-annual dynamics and drivers of salinity variations in the southern Mekong Delta, Vietnam. J. Hydrol., 661: 133745 (**13 pages**).

Box, G.E.P.; Jenkins, G.M.; Reinsel, G.C.; Ljung, G.M., (2015). Time series analysis: Forecasting and control. 5th Edn. John Wiley and Sons, New Jersey, USA. (**712 pages**).

Chan, J.C.F.; Lam, B.Y.K.; Dudgeon, D.; Liew, J.H., (2025). Global consequences of dam-induced river fragmentation on diadromous migrants: A systematic review and meta-analysis. Biol. Rev., 100(5): 2020–2037 (**18 pages**).

Dede, M.; Sunardi, S.; Lam, K.C.; Withaningsih, S., (2023). Relationship between landscape and river ecosystem services. Global J. Environ. Sci. Manage., 9(3): 637–652 (**16 pages**).

Dimitriadou, S.; Nikolakopoulos, K.G., (2022). Multiple linear regression models with limited data for the prediction of reference evapotranspiration of the Peloponnese, Greece. Hydrology, 9(7): 124 (**18 pages**).

Evans, J.D., (1996). Straightforward Statistics for the Behavioral Sciences. Brooks/Cole Publishing Company, Pacific Grove, CA, USA (**600 pages**).

Government of Indonesia, (2011). Government Regulation No. 38/2011 concerning Rivers (Peraturan Pemerintah No. 38 Tahun 2011 tentang Sungai). State Secretariat of the Republic of Indonesia, Jakarta.

Grill, G.; Lehner, B.; Thieme, M.; Geenen, B.; Tickner, D.; Antonelli, F.; Babu, S.; Borrelli, P.; Cheng, L.; Crochetiere, H.; Ehalt Macedo, H.; Filgueiras, R.; Goichot, M.; Higgins, J.; Hogan, Z.; Lip, B.; McClain, M.E.; Meng, J.; Mulligan, M.; Nilsson, C.; Olden, J.D.; Opperman, J.J.; Petry, P.; Reidy Liermann, C.; Sáenz, L.; Salinas-Rodríguez, S.; Schelle, P.; Schmitt, R.J.P.; Snider, J.; Tan, F.; Tockner, K.; Valdujo, P.H.; van Soesbergen, A.; Zarfl, C., (2019). Mapping the world's free-flowing rivers. Nature, 569(7755): 215–221 (**7 pages**).

Gupta, A.; Kumar, A., (2022). Two-step daily reservoir inflow prediction using ARIMA-machine learning and ensemble models. J. Hydro-Environ. Res., 45: 39–52 (**14 pages**).

Gupta, H.V.; Kling, H.; Yilmaz, K.K.; Martinez, G.F., (2009). Decomposition of the mean squared error and NSE performance criteria: Implications for improving hydrological modelling. J. Hydrol., 377(1–2): 80–91 (**12 pages**).

Hasan, K.; Islam, M.S.; Mitu, K.N.; Salam, M.I.; Aghashahi, N., (2025). Evaluating the performance of CHIRPS and CPC precipitation data for streamflow

forecasting using multiple linear regression and Long Short-Term Memory Neural Network model. MethodsX, 15: 103443 (**15 pages**).

Huang, B.; Peng, T.; Fan, T.; Singh, V.P.; Dong, X.; Lin, Q.; Chang, W.; Liu, J.; Huang, Y.; Guo, J.; Li, Y.; Yu, D., (2026). Assessment of dynamic drought risk and transition characteristics by combining an indicator-based approach and Markov chain model. Nat. Hazards, 122(4): 141 (**29 pages**).

Ilmi, M.K., (2022). Determination of environmental flow in Dodokan watershed based on Tennant and flow duration curve (FDC) method. Media Ilm. Tek. Sip, 10(2): 115-123 **(9 pages)**.

Irwandi, H.; Rosid, M.S.; Mart, T., (2021). The effects of ENSO, climate change and human activities on the water level of Lake Toba, Indonesia: A critical literature review. Geosci. Lett., 8(21): 1-13 (**13 pages**).

Jayanti, M.; Sabar, A.; Ariesyady, H.D.; Marselina, M.; Qadafi, M., (2023). A comparison of three water discharge forecasting models for monsoon climate region: A case study in Cimanuk-Jatigede watershed, Indonesia. Water Cycle, 4: 17-25 **(9 pages).**

Jayanti, M.; Marganingrum, D.; Plamonia, N.; Santoso, H.; Marselina, M.; Ariesyady, H.D.; Sabar, A., (2025). The operation optimization of multipurpose reservoir between ARIMA, continuous, and Markov Chain models on Jatigede reservoir, Indonesia. Water Cycle, 6: 399–411 (**13 pages**).

Jehanzaib, M.; Shah, S.A.; Yoo, J.; Kim, T.-W., (2020). Investigating the impacts of climate change and human activities on hydrological drought using non-stationary approaches. J. Hydrol., 588: 125052 (**16 pages**).

KOICA, (2006). Hydrology study: Main report - Feasibility study for Karian multipurpose dam project. Korea International Cooperation Agency and Directorate General of Water Resources, Ministry of Public Works, Seoul and Jakarta. (**185 pages**).

Kratzert, F.; Klotz, D.; Herrnegger, M.; Sampson, A.K.; Hochreiter, S.; Nearing, G.S., (2019). Toward improved predictions in ungauged basins: Exploiting the power of machine learning. Water Resour. Res., 55(12): 11344–11354 (**11 pages**).

Künsch, H.R., (1989). The jackknife and the bootstrap for general stationary observations. *Ann. Statist.*, 17(3): 1217-1241 (**25 pages**).

Li, C.; Zhu, T., (2025). Integrating Eco-Index and Hydropower Optimization for Cascade Reservoir Operations in the Lancang–Mekong River Basin. Water. 17(20): 2966 (**19 pages**).

Loucks, D.P.; van Beek, E., (2017). Water resource systems planning and management: an introduction to methods, models, and applications. Springer, Cham (624 pages)**.**

Lewis, C.D., (1982). Industrial and business forecasting methods. Butterworths, London, United Kingdom (**143 pages**).

Magar, R.B.; Jothiprakash, V., (2011). Intermittent reservoir daily-inflow prediction using lumped and distributed data multi-linear regression models. J. Earth Syst. Sci., 120(6): 1067-1084 (**18 pages**).

Margini, N.F.; Anwar, N.; Wardoyo, W.; Prastyo, D.D.; Yusop, Z., (2022). Monthly inflow forecasting of three multi-purpose reservoirs. Int. J. Adv. Sci. Eng. Inf. Technol., 12(6): 2190-2195 (**6 pages**).

Marselina, M.; Sabar, A.; Salami, I.R.S.; Marganingrum, D., (2016). Management optimization of Saguling reservoir with Bellman dynamic programming and "Du Couloir" iterative method. Forum Geografi, 30(1): 14-23 (**10 pages**).

Marselina, M.; Sabar, A.; Salami, I.R.S.; Marganingrum, D., (2017). Model prakiraan debit air dalam rangka optimalisasi pengelolaan Waduk Saguling-Kaskade Citarum. J. Tek. Sip., 24(1): 99-108 (**10 pages**).

Mazvimavi, D.; Kapangaziwir, E.; Gumbo, A.D., (2024). Assessing the effects of non-stationarity on reservoir yield estimations: A case study of the Southern Okavango Integrated Water Development system in Botswana. River Res. Appl., 40(1): 3–13 **(11 pages).**

McMahon, T.A.; Adeloye, A., (2005). Water resources yield. Water Resources Publications, Colorado, USA. (**234 pages**).

Mitze, F.; Jacobs, S.R.; Breuer, L.; Campos Zeballos, J.; Weeser, B., (2025). Evaluating hydrological model performance using varying amounts of participatory monitoring water level data. PLOS Water, 4(9): e0000405 **(21 pages)**.

Moriasi, D.N.; Arnold, J.G.; Van Liew, M.W.; Bingner, R.L.; Harmel, R.D.; Veith, T.L., (2007). Model evaluation guidelines for systematic quantification of accuracy in watershed simulations. *Trans. ASABE*, 50(3): 885-900 (**16 pages**).

Mulyawati, I.; Siti Salami, I.R.; Marselina, M.; Sabar, A., (2024). The development of inflow discharge for the karian multipurpose reservoir in the pursuit of reservoir management optimization. E3S Web Conference, 485: 04009 (**13 pages**).

Mulyawati, I.; Salami, I.R.S.; Marselina, M.; Sabar, A., (2025). A comparison of Markov Chain, Sarima and multiple linear regression for forecasting discharge. Int. J. Innov. Res. Sci. Stud., 8(3): 4176-4188 **(13 pages).**

Null, S.E.; Zeff, H.; Mount, J.; Gray, B.; Sturrock, A.M.; Sencan, G.; Dybala, K.; Thompson, B., (2024). Storing and managing water for the environment is more efficient than mimicking natural flows. Nat. Commun., 15(1): 5462 (**13 pages**).

Poff, N.L.; Richter, B.D.; Arthington, A.H.; Bunn, S.E.; Naiman, R.J.; Kendy, E.; Acreman, M.; Apse, C.; Bledsoe, B.P.; Freeman, M.C.; Henriksen, J.; Jacobson, R.B.; Kennen, J.G.; Merritt, D.M.; O'Keeffe, J.H.; Olden, J.D.; Rogers, K.; Tharme, R.E.; Warner, A., (2010). The ecological limits of hydrologic alteration (ELOHA): A new framework for developing regional environmental flow standards. Freshwater Biol., 55(1): 147–170 (**24 pages**).

Qiu, H.; Chen, H.; Xu, B.; Liu, G.; Huang, S.; Nie, H.; Xie, H., (2024). Multiple types of missing precipitation data filling based on ensemble artificial intelligence models. Water, 16(22): 3192 (**18 pages**).

Rezaeianzadeh, M.; Stein, A.; Cox, J.P., (2016). Drought forecasting using Markov chain model and artificial neural networks. Water Resour. Manag., 30(7): 2245–2259 (**15 pages**).

Rippl, W., (1883). The capacity of storage-reservoirs for water-supply. Proc. Inst. Civ. Eng., 71: 270–278 (**9 pages**).

Simeone, C.E.; Hammond, J.C.; Archfield, S.A.; Broman, D.P.; Condon, L.E.; Eldardiry, H.; Olson, C.G.; Steyaert, J.C., (2024). Declining reservoir reliability and increasing reservoir vulnerability: Long-term observations reveal longer and more severe periods of low reservoir storage for major United States reservoirs. Geophys. Res. Lett., 51(16): e2024GL109476 **(12 pages)**.

Sedghi-Asl, M.; Poursalehan, S.-J., (2025). Hydro-environmental flow classification of rivers (case study: Beshar River, Iran). Ecol. Indic., 178: 114049 (**13 pages**).

Shekohideh, H.; Vafakhah, M.; Sadeghi, S.H.R.; Moosavi, V., (2026). Evaluating the reliability, resilience, and vulnerability of water resources: the impact of minimum, maximum, environmental flows, and water quality. Appl. Water Sci., 16(8): 1-22 **(22 pages)**.

Sriwongsitanon, N.; Kaprom, C.; Tantisuvanichkul, K.; Prasertthonggorn, N.; Suiadee, W.; Bastiaanssen, W.G.M.; Williams, J.A., (2023). The Combined Power of Double Mass Curves and Bias Correction for the Maximisation of the Accuracy of an Ensemble Satellite-Based Precipitation Estimate Product. Hydrology, 10(7): 154 (**21 pages**).

Tennant, D.L., (1976). Instream flow regimens for fish, wildlife, recreation and related environmental resources. Fisheries, 1(4): 6–10 (**5 pages**).

Wahyono, H.D.; Santoso, A.D.; Goh, G.G.G.; Setiaji, G.; Salim, M.A.; Kustianto, I.; Alhasa, K.M.; Yudo, S.; Sudinda, T.W., (2026). An integrated real-time water quality monitoring system for sustainable management in tropical reservoirs. Global J. Environ. Sci. Manage., 12(2): 873–896 (**24 pages**).

Wang, M.; Wyatt, B.M.; Ochsner, T.E., (2023). Accurate statistical seasonal streamflow forecasts developed by incorporating remote sensing soil moisture and terrestrial water storage anomaly information. J. Hydrol., 626: 130154 **(39 pages)**.

Wu, H.; Tu, X.; Chen, X.; Singh, V.P.; Alfonso, L.; Lin, K.; Liu, Z.; Lai, R., (2023). A framework for water supply regulation in coastal areas by avoiding saltwater withdrawal considering upstream streamflow distribution. Sci. Total Environ., 905: 167181 (**17 pages**).

Yang, T.; Asanjan, A.A.; Welles, E.; Gao, X.; Sorooshian, S.; Liu, X., (2017). Developing reservoir monthly inflow forecasts using artificial intelligence and climate phenomenon information. Water Resour. Res., 53(4): 2786–2812 (**27 pages**).

Yang, Y.; Roderick, M.L.; Yang, D.; Wang, Z.; Ruan, F.; McVicar, T.R.; Zhang, S.; Beck, H.E., (2021). Streamflow stationarity in a changing world. Environ. Res. Lett., 16: 064096 (**9 pages**).

Yajure-Ramírez, C.A., (2026). Hydropower generation forecasting in regulated systems using two-stage feature selection. Acad. Green Energy, 3(1): 1-8 **(8 pages)**.

Yaseen, Z.M.; Karami, H.; Ehteram, M.; Mohd, N.S.; Mousavi, S.F.; Hin, L.S.; Kisi, O.; Farzin, S.; Kim, S.; El-Shafie, A., (2018). Optimization of reservoir operation using new hybrid algorithm. KSCE J. Civil Eng., 22(11): 4668–4680 (**13 pages**).

Zarei, M.; Bozorg-Haddad, O.; Baghban, S.; Delpasand, M.; Goharian, E.; Loáiciga, H.A., (2021). Machine-learning algorithms for forecast-informed reservoir operation (FIRO) to reduce flood damages. Sci. Rep., 11(1): 24295 (**21 pages**).

AUTHOR (S) BIOSKETCHES

I. Mulyawati., Ph.D. Candidate, Environmental Engineering Graduate Program, Faculty of Civil and Environmental Engineering, Institut Teknologi Bandung, Jl. Ganesha 10, Bandung 40132, Indonesia
- Email: *ira_mulyawati@usahid.ac.id*
- ORCID: 0000-0003-1589-0715
- Web of Science ResearcherID: QTU-9749-2026
- Scopus Author ID: 58893875300
- Homepage: https://usahid.ac.id/jabatan/wakil-ketua-program-studi-teknik-lingkungan/

I.R.S. Salami., Ph.D., Professor, Department of Environmental Engineering, Faculty of Civil and Environmental Engineering, Institut Teknologi Bandung, Jl. Ganesha 10, Bandung 40132, Indonesia
- Email: *indahrss@itb.ac.id*
- ORCID: 0000-0003-4108-1110
- Web of Science ResearcherID: DAAD-8781-2020
- Scopus Author ID: 25628844800
- Homepage: https://itb.ac.id/staf/profil/indah-rachmatiah-siti-salami

M. Marselina., Ph. D., Associate Professor, Department of Environmental Engineering, Faculty of Civil and Environmental Engineering, Institut Teknologi Bandung, Jl. Ganesha 10, Bandung 40132, Indonesia
- Email: *mariana.marselina@yahoo.com*
- ORCID: 0000-0002-6441-8639
- Web of Science ResearcherID: MAH-0537-2025
- Scopus Author ID: 56114581600
- Homepage: https://itb.ac.id/staf/profil/mariana-marselina-s

A. Sabar., Ph.D., Professor, Department of Environmental Engineering, Faculty of Civil and Environmental Engineering, Institut Teknologi Bandung, Jl. Ganesha 10, Bandung 40132, Indonesia.
Department of Environmental Engineering, Faculty of Infrastructure and Regional Technology, Institut Teknologi Sumatera, Jl. Terusan Ryacudu, Desa Way Hui, Kecamatan Jati Agung, Kabupaten Lampung Selatan, Provinsi Lampung, Kode Pos 35365, Indonesia.
- Email: *arwinsabar@yahoo.com*
- ORCID: 0009-0003-6460-863X
- Web of Science ResearcherID: KHX-9222-2024
- Scopus Author ID: 57194021491
- Homepage: https://ftsl.itb.ac.id/kelompok-keahlian/teknologi-pengelolaan-lingkungan/ar/

HOW TO CITE THIS ARTICLE:
Mulyawati, I.; Salami, I.R.S.; Marselina, M.; Sabar, A., (2027). Inflow modeling strategies designed to enhance the ecological sustainability of hydroelectric reservoir operation planning. Global J. Environ. Sci. Manage., 13(1): 189-212.

DOI: 10.22034/gjesm.2027.01.09
URL: https://www.gjesm.net/article_735608.html